

UC Davis

UC Davis Previously Published Works

Title

Effects of a marine heatwave on adult body length of three numerically dominant krill species in the California Current Ecosystem

Permalink

<https://escholarship.org/uc/item/6tp96084>

Journal

ICES Journal of Marine Science, 79(3)

ISSN

1054-3139

Authors

Killeen, Helen
Dorman, Jeffrey
Sydeman, William
et al.

Publication Date

2022-04-29

DOI




10.1093/icesjms/fsab215

Peer reviewed



Original article

Effects of a marine heatwave on adult body length of three numerically dominant krill species in the California Current Ecosystem

Helen Killeen ^{1,2,*}, Jeffrey Dorman ³, William Sydeman ³, Connor Dibble⁴, and Steven Morgan^{1,2}

¹Coastal and Marine Sciences Institute, University of California, 2099 Westshore Rd. Bodega Bay, Davis, CA 94923, USA

²Department of Environmental Science and Policy, University of California, One Shields Ave., Davis, CA 95616, USA

³Farallon Institute, 101 H St., Suite Q, Petaluma, CA 94952, USA

⁴Scot Science, 877 Cedar St., Suite 150, Santa Cruz, CA 95060, USA

*Corresponding author: tel: +1 (707) 875-1921; e-mail: hjkilleen@ucdavis.edu

Killeen, H., Dorman, J., Sydeman, W., Dibble, C., and Morgan, S. Effects of a marine heatwave on adult body length of three numerically dominant krill species in the California Current Ecosystem. – ICES Journal of Marine Science, 0: 1–14.

Received 17 March 2021; revised 12 October 2021; accepted 13 October 2021.

Krill are an abundant and globally distributed forage taxon in marine ecosystems, including the California Current Ecosystem (CCE). The role of krill in trophodynamics depends on both abundance and size (biomass), but the impact of extreme climate events on krill body size is poorly understood. Using samples collected from 2011 to 2018, we tested the hypotheses that adult body length of three krill species (*Euphausia pacifica*, *Thysanoessa spinifera*, and *Nematoscelis difficilis*) declined during the 2014–2016 Northeast Pacific marine heatwave/El Niño event due to elevated seawater temperatures, reduced upwelling, and low primary productivity. Hierarchical mixed-effects modelling showed that mean length of adult *E. pacifica* and *T. spinifera* declined and *N. difficilis* length increased during 2015. These trends differed by sex and reverted to a pre-heatwave state in 2016. Temperature, upwelling, and food availability (chlorophyll-*a* content) did not explain decreased length in 2015, but environmental drivers of length varied regionally and by sex across all years. This study documents the impact of a major marine heatwave (MHW) on adult krill length in one of the world's major upwelling systems and indicates how pelagic ecosystems may respond to increasingly frequent MHWs.

Keywords: chlorophyll, climate change, *Euphausia pacifica*, hierarchical mixed-effects models, length–frequency, *Nematoscelis difficilis*, reproduction, temperature, *Thysanoessa spinifera*, upwelling.

Introduction

Krill are an abundant and globally distributed taxon within marine ecosystems. They are opportunistic and omnivorous filter feeders that consume phytoplankton, microzooplankton, and detritus (Dilling *et al.*, 1998; Nakagawa *et al.*, 2004; Pinchuk and Hopcraft, 2007), and are in turn preyed upon by a wide variety of ecologically and economically important taxa, including fish (Field and Francis, 2006; Thayer *et al.*, 2014), seabirds (Hipfner, 2009), mammals (Nickels, *et al.*, 2018; Barlow, *et al.*, 2020), and invertebrates (Trathan and Hill, 2016). In the California Current

Ecosystem (CCE), a highly productive upwelling region extending from British Columbia to Baja California peninsula, krill comprise a substantial portion of the prey biomass and support productive, economically valuable fisheries (Field *et al.*, 2006; see update by Koehn *et al.*, 2016). A total of three species are particularly abundant in this region and occupy different cross-shelf and latitudinal habitats: *Euphausia pacifica* is found in greatest densities on the outer continental shelf (Brinton, 1962), *Thysanoessa spinifera* is mostly limited to the inner continental shelf north of 34.5°N (Brinton, 1962), and *Nematoscelis difficilis* is abundant throughout the Southern California Bight and is more oceanic in distribution

north of 34.5°N (Brinton, 1960). All three are crucial to CCE food-webs. Thus, understanding variation in their biomass is valuable for interpreting ecosystem-wide phenomena, predicting fisheries yields (Wells *et al.*, 2016), and evaluating changes and die-offs of seabirds and other marine predators (e.g. Sydeman *et al.*, 2015; Jones *et al.*, 2018).

Biomass is the product of abundance (ind./m³) and body size (mg/ind.). Extensive observational and laboratory research has identified drivers of changes in krill abundance and body size (growth) in the CCE. For instance, both krill abundance and growth have been positively linked to coastal upwelling (Shaw *et al.*, 2010; García-Reyes *et al.*, 2014). Upwelled, nutrient-rich water drives primary production and cools surface waters on the shelf, favouring higher phytoplankton biomass. Chlorophyll-*a* (chl-*a*), a proxy for phytoplankton abundance, is positively correlated with krill abundance (Lavaniegos *et al.*, 2019; Cimino *et al.*, 2020) and growth (Pinchuk and Hopcraft, 2007; Shaw *et al.*, 2010; Robertson and Bjorkstedt, 2020). Seawater temperature is inversely related to both krill abundance and growth (Marinovic and Mangel, 1999; Lavaniegos *et al.*, 2019; Cimino *et al.*, 2020), and may even lead to negative growth (apparent shrinkage) at temperatures > 19°C (Marinovic and Mangel, 1999). Finally, large-scale climate oscillations are also known to influence krill abundance in the CCE, including the 2- to 7-year frequency El Niño Southern Oscillation (ENSO; Marinovic *et al.*, 2002), the Pacific Decadal Oscillation (PDO; Brinton and Townsend, 2003), and marine heatwave (MHW) conditions (Brodeur *et al.*, 2019; Cimino *et al.*, 2020), with low krill abundance occurring during warm periods.

MHWs are regional phenomena associated with prolonged anomalously warm sea surface temperatures and can have a profound impact on ecosystems (Hobday *et al.*, 2016). In the CCE, a severe MHW, called the Northeast Pacific Blob, originated in late 2013 and lasted through fall 2016 (Gentemann *et al.*, 2017). Anomalously high sea level pressure in the North Pacific led to warm SST anomalies in the northern CCE beginning in spring and summer 2014 (Bond *et al.*, 2015). These conditions persisted through 2015 and into 2016, but were intensified by the 2015–2016 El Niño (DiLorenzo and Mantua, 2016) and aggravated by a delayed, weakened 2015 upwelling season (Gentemann *et al.*, 2017). The 2014–2016 MHW was associated with substantial and pervasive ecosystem-wide effects, including a reduction in the abundance of krill (Brodeur *et al.*, 2019; Cimino *et al.*, 2020). However, the impact of MHWs on krill body size has not been well-documented (except see Robertson and Bjorkstedt, 2020) despite its importance for understanding mechanisms underlying observed die-offs of krill predators (Jones *et al.*, 2018; Piatt *et al.*, 2020) and shifts in their foraging behaviour (Barlow *et al.*, 2020; Santora *et al.*, 2020). Understanding krill size response to MHWs may aid in predicting the response of zooplankton communities to future extreme events in the region and globally, which are expected to increase in frequency with climate change (Frölicher *et al.*, 2018).

To better understand the effect of MHWs on krill body size in the CCE, we examined drivers of spatial and temporal variability in adult krill length using samples collected by the NOAA-NMFS Rockfish Recruitment and Ecosystem Assessment Survey (RREAS) throughout the California portion of the CCE from 2011 to 2018 (Sakuma *et al.*, 2016), spatially expanding on prior work conducted at regional scales (Robertson and Bjorkstedt, 2020). This period includes both positive and negative ENSO phases as well as conditions before, during, and after the 2014–2016 MHW dominated the system. We hypothesized that (a) krill body length declined during

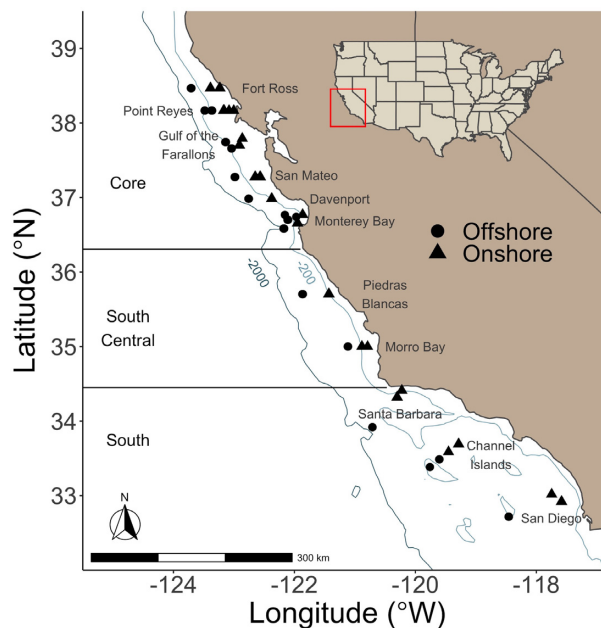


Figure 1. Points show the location of sampling stations and transects included in the study. Point shape denotes whether the station was designated as an “offshore” or “onshore” location. -200 m and -2000 m isobaths are shown in light and dark blue, respectively.

2014–2016, and (b) this was due to a combination of anomalously high temperatures, below average upwelling, and low food availability. To test these hypotheses, we modelled variability in the length of adults of three krill species (*E. pacifica*, *T. spinifer*, and *N. difficilis*) interannually and across a range of environmental conditions in 2015, during the peak of the MHW, and throughout the time series. In attempting to identify environmental drivers of MHW effects on krill body size, this work aims to inform expectations for MHWs beyond the 2014–2016 Northeast Pacific event.

Material and methods

NMFS juvenile rockfish survey

Krill samples were obtained from the RREAS. Generally, annual surveys were conducted from May through mid-June, with krill sampling occurring at night. We examined specimens collected from 2011 through 2018, except for 2014 (samples unavailable), from three of the five RREAS regions (core, south central, and south; Sakuma *et al.*, 2016) each with distinct oceanographic regimes (Checkley and Barth, 2009). In each region, RREAS sampling was conducted along multiple transects, each with stations spanning the continental shelf and slightly beyond. To characterize cross-shelf krill communities, we chose one station onshore (generally <200 m deep, ~3 km from shore) and one offshore (generally >200 m, ~45 km from shore) from each transect line (Figure 1; station metadata are available in Supplementary Table S1). Krill were sampled using a modified Cobb midwater trawl with a 26 m head-rope and 9.5 mm mesh codend. This mesh size was used to target juvenile fish (Sakuma *et al.*, 2006) and did not adequately sample krill smaller than 10 mm. Krill larvae transition to adults at 10–11 mm in length (Brinton and Wyllie, 1976; Tanasichuk, 1998a), so most larvae and some small adults were likely excluded by extrusion through the 9.5 mm mesh codend. To account for size selectivity of

our gear, we omitted all krill <10 mm from our dataset and limit our analysis to adults. While this could result in overestimation of population mean lengths, we expect this effect is negligible and unlikely to impact comparisons among samples collected using identical methods. Krill were preserved in 10% buffered formaldehyde to minimize body shrinkage of specimens during storage (Krag *et al.*, 2014).

Krill lengths

Krill samples were split using a Folsom Splitter to aliquots of the original 200 ml RREAS sample volume depending on the number of krill in the sample. All individuals in the aliquot were identified to species and sex using a dissecting microscope and a key for Pacific euphausiid identification (Baker *et al.*, 1990; Brinton *et al.*, 2000). To ensure that enough individuals were measured to create representative length frequency distributions, we sought to identify at least (1) 90 of the most common species and (2) 40 of the second most common species in each sample, and continued identifying intact individuals from successive aliquots until we had achieved both benchmarks. We excluded samples from our analysis in cases where we were unable to measure at least 40 individuals of a given species. Once identified and sexed, krill were placed on a petri dish, alongside a ruler for scale, and photographed using a Canon EOS 3000N camera. We used ImageJ (Reuden *et al.*, 2017) to measure adult krill total length using the segmented line tool along the dorsal side of the body from the foremost part of the carapace, generally the tip of the rostrum, to the most posterior point on the telson (Brinton and Wyllie, 1976).

Environmental predictors

To model adult krill length, we chose predictor variables for environmental models of length based on our hypotheses and drivers that likely impact adult krill body size in the CCE, including seawater temperature, food availability, upwelling, and ocean climate (Table 1). We accounted for daily vertical migrations (on day-night cycles) for all three species by using both temperature at 2 m depth (sea surface temperature; SST) and temperature at 100 m depth (subsurface temperature) to represent conditions affecting krill. Mean daily surface and subsurface temperatures were extracted from the Regional Ocean Modelling System (ROMS) Nowcast (10 km resolution) for each station using the virtual sensor tool available on the CenCOOS Data Portal (<https://data.cencoos.org/>). Daily mean satellite chl-*a* values (4 km² minimum spatial resolution) were extracted for each station via the THREDDS data server from the European Space Agency Ocean Color Climate Change Initiative (version 4.2; accessible at <https://rsg.pml.ac.uk/thredds/>) and log transformed (Sathyendranath *et al.*, 2020). In addition to chl-*a*, we tested the impact of the standard deviation of SST (SST *SD*) on krill length, which may be an indicator of food availability as a proxy for the horizontal presence of fronts and has been associated with *T. spinifera* abundance in the region (Cimino *et al.*, 2020). SST *SD* values were assigned to each station by taking the standard deviation of ROMS 2 m temperatures over a chosen period prior to sampling (see below). We used the daily Cumulative Upwelling Transport Index (CUTI; accessed at <http://mjacox.com/upwelling-indices/>) as an indicator of regional coastal upwelling intensity and duration at each station. CUTI incorporates vertical transport due to both Ekman flux and cross-shore geostrophic transport, providing a local (1° latitude, 0–75 km from shore) estimate of recent upwelling

conditions experienced by krill prior to collection (Jacox *et al.*, 2018). Finally, we included the multivariate ocean climate index (MOCI; accessed at <http://www.faralloninstitute.org/moci>) as a measure of regional ocean conditions and low-frequency climate oscillation (see García-Reyes and Sydeman, 2017 for details). Each station was assigned the corresponding MOCI value for its region (MOCI regions: north, central, and southern California) during the spring months (April–June). High (low) MOCI values are indicative of warm (cold) and low (high) productivity conditions in the CCE.

To determine the number of days over which to average each predictor, we modelled adult krill length against each predictor averaged over increasing durations (1–30 days) such that length~predictor_{*i*}, where *i* is the number of days over which the predictor was averaged. We chose a value for *i* by selecting the model with the highest *R*² for a given predictor (Supplementary Figure S2). All environmental predictors and krill length were scaled (means and variances equate to 0 and 1, respectively) for analysis and interpretation.

Modelling

Statistical modelling of lengths was conducted in R version 3.6.2 (R Core Team, 2019) using a hierarchical linear mixed modelling approach with varying intercepts. This method allowed us to examine the effects of interannual variation and environmental predictors on body length of adult krill throughout the CCE while accounting for differences in the effect of sampling location (Gelman and Hill, 2007). We designed three families of models to examine (i) interannual variability in adult krill length; (ii) the role of upwelling, SST, and chl-*a* in determining adult krill length during the peak of the MHW in 2015; and (iii) environmental drivers of spatial and temporal variability in adult krill length throughout our time series (Table 1). All models were constructed using the lme4 package (Bates *et al.*, 2015), and figures and tables were made using the packages ggplot2 (Wickham, 2016), superheat (Barter and Yu, 2017), and kableExtra (Zhu, 2020). Data and analyses are publicly available online (<https://doi.org/10.17605/osf.io/c8hr3>).

To test our first hypothesis that mean adult krill length declined during 2014–2016, we constructed two sets of mixed-effect models with a variable intercept for station. The first set of models included sex as a predictor to determine whether sexes were impacted differently by year. The second set did not include sex as a predictor to estimate the effect of year on adult krill length across males and females. Both sets included one model for each of the three species. Model structure followed the form (Gelman and Hill, 2007):

$$l_i = \alpha_{j|i} + X_i\beta + \epsilon_i$$

$$\text{where } \alpha_j \sim N(\mu_\alpha, \sigma_\alpha^2)$$

$$\text{and } \epsilon_i \sim N(0, \sigma^2),$$
(1)

where *l* is a vector of length *n*, representing standardized krill lengths for *n* individuals, indexed as *i*. *α* is a vector of random intercepts associated with station *j* and is normally distributed with a mean of *μ_α* and variance of *σ_α²*. *X* is the matrix (*n* × *p*) for *p* fixed-terms of year, sex, and year by sex interaction. *β* is the vector (*p* × 1) of fixed-term coefficients and *ε* is the vector (*n* × 1) of error terms with a zero mean and variance of *σ²*.

To test our second hypothesis that changes in mean adult krill length during the MHW were driven by upwelling, SST, and chl-*a*, we constructed species-specific mixed-effects models of krill length

Table 1. Environmental and biological predictors and grouping factors included in linear mixed-effects models of krill body length off California from 2011 to 2018. Temporal and spatial averaging columns indicate the domain over which predictors were averaged. *Chl-*a* values were accessed from the Ocean Color Initiative, which merges multiple satellite chlorophyll products with variable (4 km² minimum) spatial resolution.

Predictor	Variable	Description	Purpose	Temporal Averaging	Spatial Averaging	Source
Sea surface temperature	temp_2	Temperature at 2 m depth	Direct impact of temperature on body size	10 days	10 km ²	Regional Ocean Modelling System 10 km Nowcast
Subsurface temperature	temp_100	Temperature at 100 m depth	Direct impact of temperature on body size	5 days	10 km ²	Regional Ocean Modelling System 10 km Nowcast
SST standard deviation	sst_sd	Standard deviation of temperature at 2 m depth	Food availability	17 days	10 km ²	Regional Ocean Modelling System 10 km Nowcast
Chlorophyll- <i>a</i>	chl- <i>a</i>	Log chlorophyll- <i>a</i> content	Food abundance	27 days	4 km ² *	Sathyendranath <i>et al.</i> (2020)
Multivariate ocean climate index	Moci	Multivariate index capturing regional atmospheric and oceanographic variability	Regional, seasonal oceanographic variability including low-frequency oscillations	3 months	Regional	García-Reyes and Sydeman (2017)
Coastal upwelling transport index	Cuti	Local upwelling strength as a function of Ekman and geostrophic transport	Local upwelling intensity	9 days	1 degree latitude	Jacox <i>et al.</i> (2018)
Sex	Sex	Krill sex	Sexual dimorphism	NA	NA	NA
Station	Station	Station number	Grouping variable for random intercept and regression estimation, captures station-level variation in habitat type, and distance from shore	NA	NA	RREAS

with varying intercepts for each of 3 years before (2013, average MOCI = -1.28), during (2015, average MOCI = 1.41), and after (2017, average MOCI = 0.77) the MHW. We also examined differences in the impact of predictors on male and female krill by including interaction terms of sex and environmental predictors in the 2015 model. Model structure used the same form as Equation (1), where X is the matrix ($n \times p$) for p fixed terms of SST, upwelling, chl-*a*, sex, and their two-way interactions terms.

To explore environmental drivers of adult krill length more generally across the whole time series, and to investigate regional variability in drivers of adult krill size, we constructed three species-specific mixed-effects models with varying intercepts and slopes. Model structure followed the form (Gelman and Hill, 2007):

$$l_i \sim N(\alpha_{j[i]} + \gamma_{j[i]}\tau_i + X_i\beta, \sigma^2), \text{ for } i = 1, \dots, n$$

$$\text{where } \begin{pmatrix} \alpha_j \\ \gamma_j \end{pmatrix} \sim N\left(\begin{pmatrix} \mu_\alpha \\ \mu_\gamma \end{pmatrix}, \begin{pmatrix} \sigma_\alpha^2 & \rho\sigma_\alpha\sigma_\gamma \\ \rho\sigma_\alpha\sigma_\gamma & \sigma_\gamma^2 \end{pmatrix}\right), \text{ for } j = 1, \dots, J,$$

(2)

where α is an intercept estimated for each station j , γ_j is the station-specific SST coefficient, and τ is SST. X is a matrix ($n \times p$) containing vectors for sex, the set of environmental predictors described in Table 1, and interactions between sex and environmental predictor; β is the vector ($p \times 1$) of estimated coefficient for each fixed term. Variable intercepts and slopes for station were modelled as normal distributions with means (μ_α, μ_γ) and variances ($\sigma_\alpha^2, \sigma_\gamma^2$) including a between-station correlation parameter, ρ . We excluded

fixed terms from species-specific models of environmental drivers across the whole time series in two cases based on data structure considerations. First, we excluded subsurface temperature from the *T. spinifera* model because a large proportion of individuals were collected at stations with depths ≤ 100 m (37%). Second, the term $\gamma_{j[i]}\tau_i$ was left out of the *N. difficilis* model because too few individuals were measured to estimate station-specific temperature coefficients. We used an information theoretic approach (Grueber *et al.*, 2011) and the MuMIn package (Bartón, 2020) to select a single top-performing model for each species. Model performance was evaluated by comparing Akaike Information Criterion (AIC) values associated with each fixed and random effect structure. We selected the model with the lowest AIC value. Collinearity was assessed graphically and by calculating the variance inflation factor associated with each top-performing model.

RESULTS

We measured 11284 *E. pacifica*, 5865 *T. spinifera*, and 1636 *N. difficilis* individuals (total $n = 18785$). Table 2 shows count data for krill included in the analysis by species, sex, year, and region. Mean length of adult krill varied by species. The mean length of adult *E. pacifica* was 20.92 mm with a 95% confidence interval (CI) of 20.87–20.96 mm; adult *T. spinifera* mean length was 24.06 mm (CI: 23.97–24.16 mm); and adult *N. difficilis* mean length was 22.41 mm (CI: 22.27–22.55 mm). After confirming that the distributions of

Table 2. Sample size of krill measured for each year and region off California from 2011 to 2018, with totals in the bottom row. Columns show species and sex totals for the core (C), south central (SC), and south (S) regions as defined in Figure 1.

Year	<i>E. pacifica</i>						<i>T. spinifera</i>						<i>N. difficilis</i>					
	Female			Male			Female			Male			Female			Male		
	C	SC	S	C	SC	S	C	SC	S	C	SC	S	C	SC	S	C	SC	S
2011	1250	55	0	732	58	0	565	67	0	667	22	0	31	0	0	16	0	0
2012	538	131	545	396	38	302	554	58	169	235	12	84	37	0	44	23	0	1
2013	553	0	0	394	0	0	582	0	0	398	0	0	49	0	0	12	0	0
2015	276	156	359	168	30	182	0	28	165	0	28	102	35	0	285	16	0	46
2016	678	241	50	457	131	36	143	0	0	164	0	0	153	59	85	21	25	15
2017	515	323	238	317	232	125	470	74	84	152	102	24	100	36	193	52	11	39
2018	737	163	266	379	67	166	435	70	19	321	21	50	0	0	232	0	0	20
Total	4 547	1 069	1 458	2 843	556	811	2 749	297	437	1 937	185	260	405	95	839	140	36	121

each species-sex were normal, a two-sample *t*-test showed that females were larger than males by 0.94 mm ($t = 6.03, p < 0.001$) for *E. pacifica* and by 2.63 mm ($t = 6.87, p < 0.001$) for *T. spinifera*. *Nematoscelis difficilis* females were 0.86 mm larger than males, but the result was not statistically significant ($t = 1.53, p = 0.14$).

Interannual variability in krill length

Total length of adult krill varied interannually for all three species. Species-specific mean length varied by year up to 9.6%, 19.5%, and 14.7% for *E. pacifica*, *T. spinifera*, and *N. difficilis*, respectively (Figure 2). We expected that krill would be smaller during 2015 and 2016 (no length data available for 2014). Results of our interannual linear mixed modelling analysis show that in 2015 *E. pacifica* and *T. spinifera* mean lengths were smaller than average, but *N. difficilis* mean length was larger than average (Figure 3a; full results available in Supplementary Tables S3–S5). From 2016 to 2018, *E. pacifica* and *T. spinifera* mean lengths were larger than average and *N. difficilis* mean length was smaller than average.

We also found that the impact of year on mean total length of adult krill differed for males and females (Figure 3b; full results available in Supplementary Tables S6–S8). In all years but 2015, mean total length of females was greater than males. In 2015, mean total length of adult males was larger than females for both *T. spinifera* and *N. difficilis*. *E. pacifica* females remained larger than males in 2015, but the species exhibited a 39% reduction in size-based sexual dimorphism relative to 2013 (Figure 3c). From 2016 onward, we observed a return to the pre-heatwave pattern of larger females and smaller males for all three species.

Environmental drivers of adult krill body length

The period when samples were collected was marked by substantial interannual environmental variability in the CCE. Cool conditions with negative MOCI values prevailed in 2011–2013 but shifted to warmer conditions by 2014 (Figure 4k and l) with the onset of the MHW. In 2015, positive MOCI values, warm surface and subsurface temperatures, and average to below average upwelling were associated with reduced chl-*a* concentrations. By the time samples were collected in 2016 (May–June), surface and subsurface temperatures as well as upwelling had begun to return to a pre-heatwave state. MOCI values declined through 2017 and 2018, and other covariates returned to average values for the study period.

Euphausia pacifica

Our hypothesis that decreases in krill length during 2014–2016 were driven by elevated SST and reduced upwelling and primary productivity was not supported for *E. pacifica*. We found that adult *E. pacifica* length was not significantly associated with SST, CUTI, or chl-*a* during 2015, and we did not observe significant differences between sexes in length response to the three predictors (Figure 5 and Table 3). When considering the impact of the environment on krill length throughout the time series (2011–2018) we found that *E. pacifica* size was moderately positively associated with increases in SST SD and moderately negatively associated with increases in CUTI and chl-*a* (Figure 6; CIs available in Supplementary Table S9). The influence of SST and subsurface temperature differed by sex, but not substantially.

We used estimated variable intercepts and slope coefficients from our model of krill length and environmental conditions (2011–2018) to interpret the effect of station on adult krill length (Figure 7a and b). Variable intercepts, which estimate mean length at each station, showed that *E. pacifica* tended to be slightly larger onshore than offshore (unpaired two-sample Wilcoxon test: $W = 99, p = 0.064$). SST variable slope coefficients, which estimate station-level differences in the response of adult krill length to changes in SST showed that krill length in the core region was more positively associated with increases in SST than in the south region (Kruskal–Wallis test: $\chi^2 = 6.92, p = 0.031$).

Thysanoessa spinifera

In 2015, *T. spinifera* body size was not associated with SST or primary productivity, but it was inversely associated with CUTI, failing to support our hypotheses for the first two variables and contradicting our hypothesis for the third (Figure 5 and Table 3). However, *T. spinifera* males showed a much weaker relationship with CUTI than females. Throughout the time series (2011–2018), lengths of adult *T. spinifera* females and, to a lesser extent, males were strongly negatively associated with increases in chl-*a*. *Thysanoessa spinifera* length was moderately positively associated with increases in SST SD. Female, but not male, length was moderately negatively associated with the MOCI (Figure 7; CI available in Supplementary Table S10). There was moderate variability in the effect of station on *T. spinifera* length (Figure 7c). Variable intercept estimates indicated that adult *T. spinifera* were smallest at the northernmost stations (Point Reyes and Fort Ross, Figure 1) but size varied little throughout the rest of the study area. Slope coefficients for SST were highly

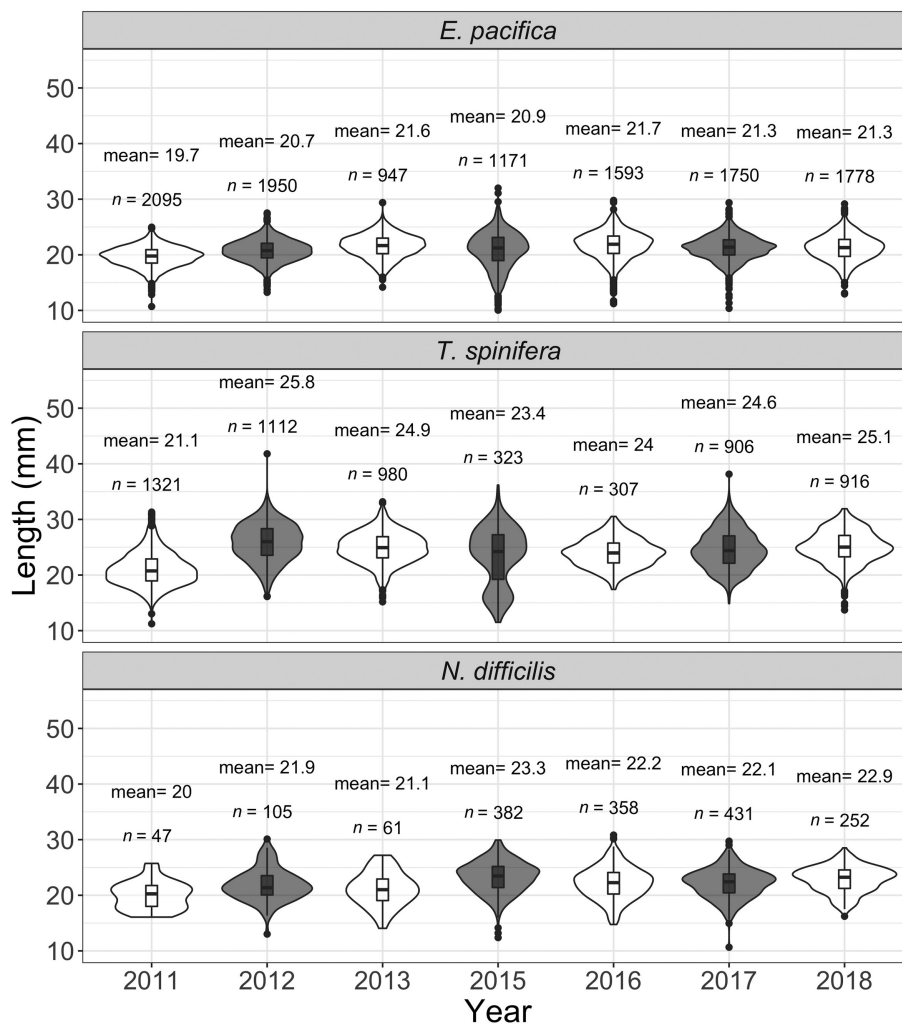


Figure 2. Raw length–frequency distributions for three krill species collected off California from 2011 to 2018. Mean values indicated by inset box-and-whisker plots.

variable. Excluding the two northernmost transects, *T. spinifera* on-shore responded more positively to increases in SST than offshore (unpaired two-sample Wilcoxon test: $W = 40$, $p = 0.05$; Figure 7d).

Nematoscelis difficilis

In 2015, adult *N. difficilis* male, but not female, length was positively associated with CUTI, partially supporting our hypothesis for the role of upwelling in determining krill size during 2014–2016. Female *N. difficilis* showed no relationship with SST but males showed a positive association, contradicting our hypothesis for the role of SST in determining krill size during the 2014–2016. Finally, only male *N. difficilis* length was positively associated with chl-*a*, partially supporting our hypothesis for primary productivity (Figure 5 and Table 3). Throughout the time series (2011–2018), adult *N. difficilis* were strongly positively associated with increases in MOCI and CUTI, and moderately positively associated with increases in chl-*a* (Figure 6; CIs available in Supplementary Table S11). However, the sample size of *N. difficilis* was considerably smaller than the other two species so model estimates may be biased. There was little variability in the effect of station on length (Figure 7e). *Nematoscelis difficilis* were only present onshore in the south region, where the

species is most abundant, and were infrequently present north of 34.5°N. Consequently, few station intercepts were estimated for the core region.

DISCUSSION

Previous warm periods in the CCE have been linked to reduced krill abundance (Brinton and Townsend, 2003; Fleming *et al.*, 2016; Cimino *et al.*, 2020), but it has been unclear how such periods have impacted krill body length, critical to understanding available biomass for krill predators in the ecosystem. Here we show some of the first evidence that (i) adult *E. pacifica* and *T. spinifera* lengths declined and adult *N. difficilis* lengths increased throughout the region during the peak of the 2014–2016 Northeast Pacific MHW and the beginning of the 2015–2016 El Niño, confirming patterns in *E. pacifica* and *T. spinifera* length observed off Trinidad Head during the same period (41°N; Robertson and Bjorkstedt, 2020); (ii) the effect of the MHW/El Niño and environmental conditions on adult krill length differed strongly by sex; and (iii) adult krill length and its response to increases in SST differed regionally and across the shelf. These results relate exclusively to adult krill > 10 mm, and it is likely that interannual variation and environmental drivers of krill

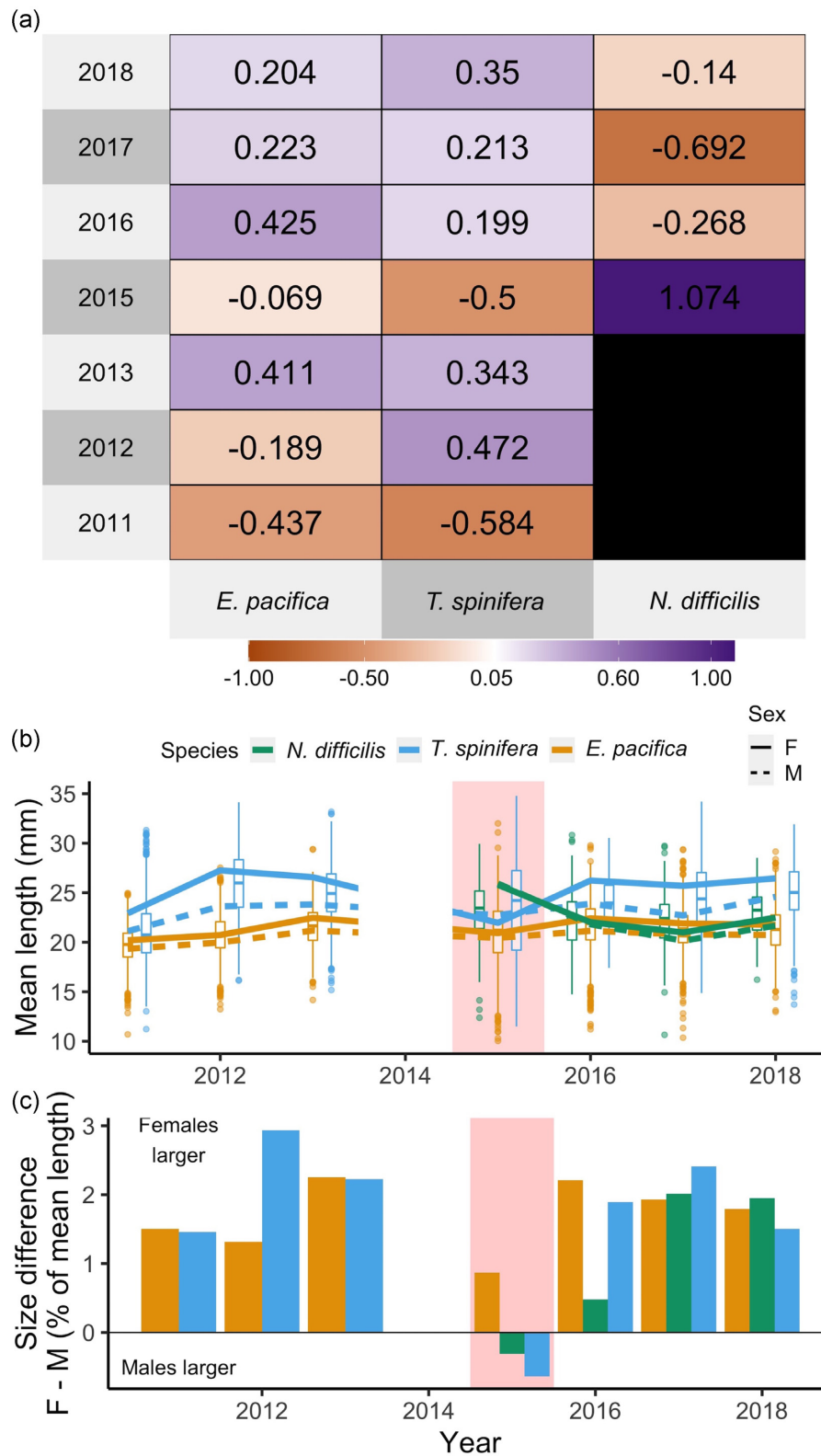


Figure 3. (a) Coefficient estimates of year impact on krill length derived from linear mixed-effects models with a variable intercept for station and fixed effects for year. Values and colours indicate deviation from the overall population mean length in units of standard deviation. Estimates for *N. difficilis* from 2011 to 2013 are not shown due to low sample size. (b and c) Simulated data from linear mixed-effects model with a variable intercept for station and fixed effects of year, sex, and year:sex. The peak of the MHW is shaded red. (C) Size difference between male and female krill across all years. Bars above the zero line indicate females were larger.

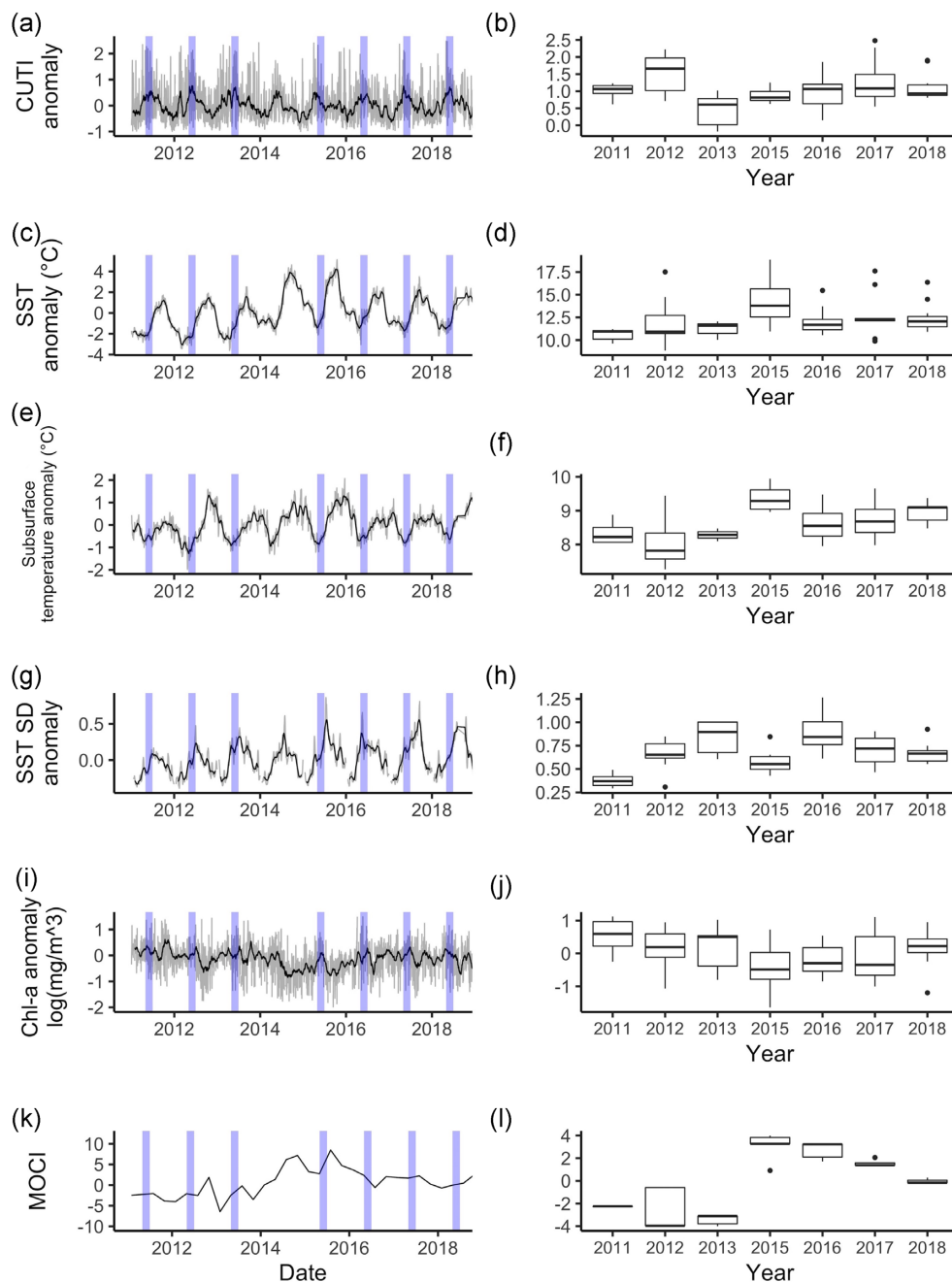


Figure 4. Time series of environmental covariates used in environmental models of krill length off California from 2011 to 2018, including CUTI (a and b), SST (c and d), subsurface temperature (e and f), SST SD (g and h), chl-*a* (i and j), and MOCI (k and l). Plots in the left column show conditions averaged across representative stations indicated in Supplementary Figure S1. The gray line shows daily average values, and the black line shows a 30-day moving average. RREAS sampling periods indicated by blue bars, excluding 2014. Boxplots in the right column show covariate values (based on timing and location of sample collection) included in linear mixed-effects models of environmental drivers of krill length.

length differ for smaller age/size classes (Robertson and Bjorkstedt, 2020). Nonetheless, as adults comprise a large portion of available krill biomass and constitute the breeding part of the population, documenting drivers of adult krill length is useful for understanding both krill trophic ecology and population dynamics.

This study indicates how extreme climate events impact krill biomass over broad spatial and temporal scales by investigating changes in mean population length. However, it is important to

note that individual growth is not the only factor that can influence mean population length. Low growth/shrinkage as well as an increase in recruitment of juveniles (small size classes) to the adult stage can reduce mean population length. For instance, we found that mean adult length was smallest during 2011 and 2015 (Figure 3a). This was surprising given that the 2 years were very different in key indicators of ocean condition (Figure 4). A strong La Niña occurred in 2011 with negative MOCI values and negative SST

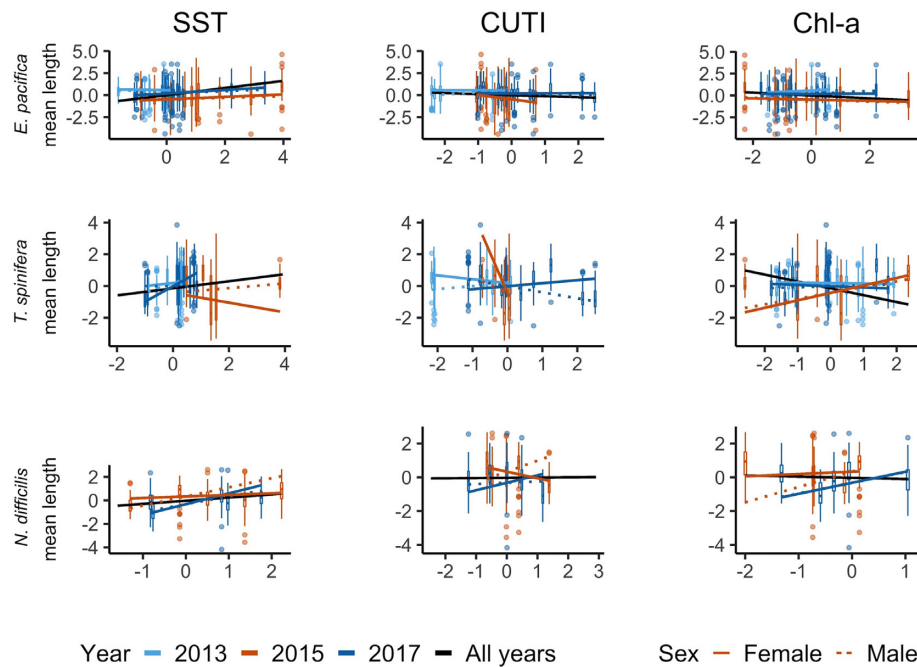


Figure 5. Annual, species-specific linear mixed-effects models of krill length with SST, CUTI, chl-*a*, and sex two-way interaction terms as fixed effects and variable intercepts for station. SST, CUTI, and chl-*a* trends are shown before the heatwave (2013, light blue line), during the heatwave (2015, orange line), after the heatwave (2017, dark blue line), and across all years (2011–2018, black line). Solid lines show trends for females and dotted lines show trends for males. Boxplots show the distribution of raw data for each year, station. All length and predictor values are standardized such that means are 0 and variances are 1.

anomalies (generally indicators for high productivity) throughout the CCE. In contrast, 2015 was characterized by positive MOCI values and some of the highest SST anomalies (generally indicators for low productivity) in the time series. Consequently, it is unlikely that shared environmental conditions across the 2 years led to low growth. High levels of spawning in early 2011 (January–March), triggered by elevated primary production, may have led to a large cohort of juveniles recruiting to the adult stage by the time RREAS sampling took place (May–June), resulting in lower mean population length of adults > 10 mm. This is supported by the observation that krill abundance was anomalously high in 2011 (Cimino *et al.*, 2020). However, in 2015, when krill abundance was anomalously low (Cimino *et al.*, 2020), low growth due to adverse environmental conditions, rather than an influx of juveniles, is more likely to have caused observed declines in population mean length. As changes in both age structure and growth are viable mechanisms for shifts in population mean length, future observational studies could expand on this work by quantifying or controlling for both processes concurrently (Shaw *et al.*, 2021).

Krill length 2014–2016

While it is unfortunate that we were not able to report on krill length in 2014, when the beginnings of the MHW were first felt in our study area, we did observe interesting differences in krill body size across 2015 and 2016. *Euphausia pacifica* and *T. spinifera* size declined dramatically in 2015 and recovered in 2016 while *N. difficilis* displayed the opposite pattern. Ocean conditions and the evolution of the MHW also differed in 2015 and 2016. Anomalously warm SSTs peaked in 2015 (Gentemann *et al.*, 2017) with the northward propagation of an El Niño and subsequent reintensification of the

MHW in the winter of 2014/15 (DiLorenzo and Mantua, 2016). *Nematoscelis difficilis* were exceptionally large during this period, perhaps due to the species' adaptation to subtropical-tropical as well as temperate waters (Brinton, 1962) and poleward advection linked to the El Niño (Lilly and Ohman, 2021). By the winter of 2015/16, SSTs in our study region were still warm but not as warm as in 2015 (Gentemann *et al.*, 2017). Moreover, in the weeks leading up to 2016 krill sampling, upwelling, and chl-*a* content were more similar to pre- and post-MHW conditions (Figure 4). Therefore, declines in *E. pacifica* and *T. spinifera* size, such as that observed in 2015, may be linked more to the intensity than the duration of extreme climate events like the MHW, and length frequency distributions may be able to recover quickly as extreme events elapse.

Length-based sexual dimorphism

Our findings confirm well-established knowledge that female krill are larger than males (Nemoto, 1966; Tanasichuk, 1998a). However, in 2015, adult female: male length ratios declined for all three species and even inverted for *T. spinifera* and *N. difficilis* (Figure 3c) driven by a disproportionate reduction in female length. Hence, conditions associated with the MHW may have disrupted energy allocation for growth by adult female krill, but not males, during or prior to sample collection (May and June).

All three species spawn in the spring and summer (Brinton and Wyllie, 1976; Feinberg and Peterson 2003), and it is expected that female krill allocate more energy towards reproduction than males during this period (Pond *et al.*, 1995; Tanasichuk, 1998b). As female krill are unlikely to be smaller from prioritizing reproductive investment over growth (see above discussion around spawning during 2015), observed reductions in female length are more likely due

Table 3. Coefficient estimates of fixed effects (SST, CUTI, chl-*a*, and sex two-way interaction) from annual, species-specific linear mixed-effects models of krill length with variable intercepts for station. Estimates shown beside 95% CIs in parentheses. Bolded values indicate estimates for which the 95% CI does not cross 0. The number of stations (variable intercepts) in each model, marginal R^2 (R^2 of model with only fixed effects), and conditional R^2 (R^2 of model with fixed and station-level effects) are shown in the three columns to the right.

Species	CUTI	SST	chl- <i>a</i>	SexCUTI	SexSST	SEX:chl- <i>a</i>	Stations	Marginal R^2	Conditional R^2
2013									
<i>E. pacifica</i>	0.01 (-0.26–0.27)	-0.05 (-0.42–0.33)	0.16 (-0.09–0.41)	0.24 (0.17–0.30)	0.10 (-0.16–0.36)	0.31 (0.12–0.39)	8	0.127	0.145
<i>T. spinifera</i>	-0.24 (-0.49–0.00)	0.18 (-0.44–0.81)	-0.03 (-0.25–0.20)	0.43 (0.37–0.50)	0.40 (0.12–0.68)	-0.03 (-0.13–0.07)	10	0.191	0.318
2015									
<i>E. pacifica</i>	-0.49 (-1.32–0.35)	0.14 (-0.19–0.47)	-0.07 (-0.38–0.24)	-0.02 (-0.28–0.25)	-0.05 (-0.18–0.07)	-0.04 (-0.17–0.09)	10	0.109	0.278
<i>T. spinifera</i>	-5.07 (-9.30–0.84)	-0.31 (-1.36–0.75)	0.47 (-0.27–1.21)	4.07 (2.90–5.33)	0.46 (0.22–0.69)	-0.11 (-0.38–0.17)	5	0.233	0.523
<i>N. difficilis</i>	-0.39 (-2.51–1.73)	-0.13 (-1.56–1.82)	0.14 (-1.77–2.05)	1.04 (0.47–1.62)	0.64 (0.10–1.18)	0.77 (0.11–1.43)	5	0.058	0.474
2017									
<i>E. pacifica</i>	0.01 (-0.11–0.13)	0.20 (0.11–0.32)	0.01 (-0.09–0.11)	-0.11 (-0.23–0.00)	-0.06 (-0.21–0.08)	0.15 (0.04–0.26)	16	0.055	0.082
<i>T. spinifera</i>	0.19 (-0.22–0.60)	0.98 (0.19–1.77)	-0.08 (-0.37–0.21)	-0.57 (-0.73–-0.41)	-1.00 (-1.27–-0.72)	0.14 (0.03–0.25)	10	0.260	0.496
<i>N. difficilis</i>	0.44 (0.11–0.78)	0.92 (0.56–1.27)	0.66 (0.36–0.95)	-0.37 (-0.85–0.12)	-0.26 (-0.76–0.24)	-0.02 (-0.40–0.35)	5	0.144	0.157

to low growth or shrinkage when food availability was low, water temperatures were high, and energy was required to sustain even very limited reproductive output. This could also help explain low krill abundance in 2015 and 2016 as smaller females tend to produce smaller brood sizes for both *E. pacifica* and *T. spinifera* (Ross and Quetin, 2000; Gómez-Gutiérrez *et al.*, 2006; Feinberg *et al.*, 2007). To evaluate the effect of extreme climate events on krill, future studies should consider the concurrent abundance, length, and reproductive state of individuals. Such an approach would be particularly helpful in differentiating between fluctuations in length due to reproductive output vs. growth, both of which are impacted by environmental change (Pinchuk and Hopcraft, 2007; Shaw *et al.*, 2021).

Environmental drivers of krill body length

Sea surface temperature

There is strong evidence that *E. pacifica* length declines with rising temperature (Robertson and Bjorkstedt, 2020), particularly when temperatures exceed 14°C and metabolic efficiency declines (Iguchi and Ikeda, 1995; Alonzo and Mangel, 2001). *Euphausia pacifica* in the CCE are even known to shrink with successive moults when *in situ* SST increases above 19°C (Marinovic and Mangel, 1999). Nonetheless, adult length in our study was not strongly associated with SST before, during, or after 2014–2016 for any of the three species (though it was strongly associated with SST SD, see Supplementary Materials). Incongruence between our findings and prior work may be because 10-day averaged surface temperature derived from a 10 km² gridded numerical ocean model (ROMS) does not adequately capture conditions experienced by krill *in situ*. However, we believe these data are a reasonable approximation of *in situ* conditions experienced by krill over the temporal scale of krill moulting, with intermoult periods on the order of several days (Marinovic and Mangle, 1999; Pinchuk and Hopcraft, 2007; Shaw *et al.*, 2010).

In 2017, mean body length of all three species increased with SST (Table 3). *Euphausia pacifica* length was also weakly positively associated with SST when we modelled length across all years (2011–2018; Figure 6). These trends directly contradict previously documented relationships between temperature and length. However, SSTs in our study domain were infrequently above the 14°C threshold identified by Iguchi and Ikeda (1995), suggesting that krill may have rarely (except in 2015) been exposed to water temperatures that directly curtail growth or cause shrinkage. In a *post hoc* test examining whether adult *E. pacifica* length exhibits a different relationship with SSTs above and below 14°C, we compared model performance of nonlinear and linear models of SST and mean *E. pacifica* length (Supplementary Figure S12). The nonlinear model showed a more positive association between SST and length at temperatures below 14°C than above the threshold. Hence, elevated SST may result in larger adult *E. pacifica* up to approximately 14°C with diminishing returns at higher SST values. Alternatively, krill species may show longer mean length with moderate SST increases as a result of reduction in reproductive effort (Feinberg *et al.*, 2007) or selective mortality of smaller individuals, but we did not quantify reproductive effort or cohort survival in our study.

Upwelling and food availability

Upwelling was not strongly linked to adult mean length in 2015 for either *E. pacifica* or *N. difficilis*, but it was strongly negatively associated with female *T. spinifera* mean length (Table 3). This latter

Environmental Predictor	temp_2	0.072	[Black Box]		
	temp_100	0.022			
	sst_sd	0.131	0.18	[Black Box]	
	chla	-0.222	-0.516		0.12
	moci_spring	0.055	-0.183	0.515	
	cuti	-0.106	0.055	0.257	
	sexM:temp_2	0.068	[Black Box]		
	sexM:temp_100	-0.051			
	sexM:chla	[Black Box]		0.049	0.17
	sexM:moci_spring	[Black Box]		0.158	0.226
	sexM:cuti	[Black Box]		0.113	
			<i>E. pacifica</i>	<i>T. spinifera</i>	<i>N. difficilis</i>

Figure 6. Estimated coefficients for environmental predictors and interactions with sex estimated by linear mixed-effects models of krill length with variable intercepts and slopes across all years (2011–2018). Values and colours show the influence of a change of one standard deviation in the predictor on standardized krill length in units of standard deviation. Coefficients for environmental predictors represent the impact of corresponding drivers on female length, while interaction coefficients show how each driver impacted males relative to females. Black boxes indicate parameters that were not used in optimized species models.

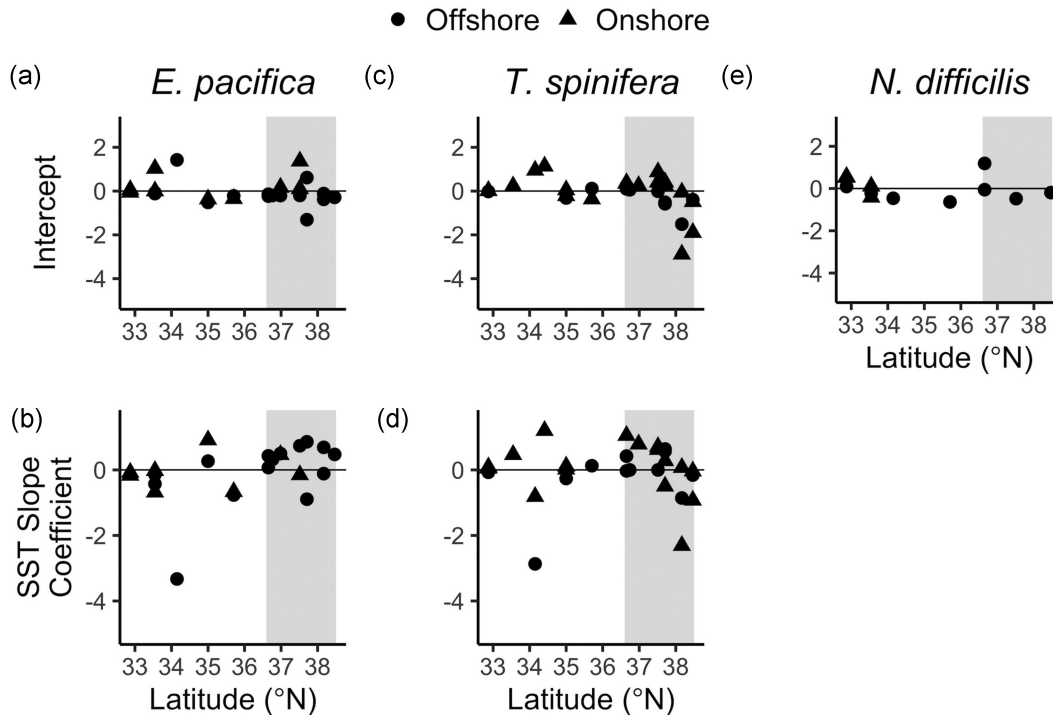


Figure 7. Station-level variable intercepts (a, c, and e) and slopes (b and d) estimated by linear mixed-effects models of environmental drivers of krill lengths across all years (2011–2018). Point share denotes offshore stations (>200 m deep, ~45 km from shore) and onshore stations (<200 m deep, ~3 km from shore). Gray shading shows the location of the core region.

trend was driven by two stations off Santa Barbara where female *T. spinifera* were substantially smaller than males following a period of typical upwelling intensity. During a year of otherwise below average upwelling, this localized pulse of upwelling may have stimulated an increase in energy allocation to reproduction by females, resulting in shrinkage or low growth of females but not males (Smiles and Pearcy, 1971; Feinberg et al., 2007).

The same process may be responsible for the strongly negative relationship observed across all years (Figure 6) between chl-*a* and mean length of *E. pacifica* and *T. spinifera*. The size of adult *E. pacifica* size tends to peak prior to spawning (Robertson and Bjorkstedt, 2020), which is timed to overlap with phytoplankton blooms, as indicated by chl-*a* content peaks (Feinberg et al., 2010; Shaw et al., 2021). Adult length may have declined with increasing chl-*a* content as a result of elevated spawning rather than lack of food (Shaw et al., 2021). It is worth noting that satellite chlorophyll-*a* content (4 km² resolution) may not be a reliable indicator of food availability for krill. Satellite derived data may differ from *in situ* concentrations, and it cannot indicate subsurface chlorophyll concentrations, which also play a role in determining food availability for vertically migrating krill (Shaw et al., 2021). In addition, chl-*a* does not reflect the full complement of food resources available to krill. As opportunistic heterotrophs, krill feed on phytoplankton, marine snow (Dilling et al., 1998), and other planktonic invertebrates (copepods; Ohman 1984), and heterotrophic feeding might ameliorate the impact of low phytoplankton availability on the body size reduction of adult krill.

Regional variation in krill body length response to temperature

A major benefit of using a mixed-effects modelling approach to examine species trends over large spatial scales is that it allowed us to look at both ecosystem-wide and local drivers of krill length. For example, *E. pacifica* and *T. spinifera* response to SST varied regionally throughout the CCE. Krill length onshore (*T. spinifera*) and in the core region (*E. pacifica*) responded more positively to increasing SSTs than in other regions (Figure 7b and d). Strong, persistent springtime upwelling yields high pelagic productivity in these zones but also cooler surface waters. Therefore, adult *E. pacifica* and *T. spinifera* body size in localities with high upwelling intensity may be limited less by food availability and more by thermal limits on metabolic efficiency (Marinovic and Mangel, 1999), allowing them to benefit from limited increases in SST. Such a mechanism would help to explain why adult krill were of average length in 2016, when SSTs were still high relative to other years in the time series but CUTI had increased relative to 2015. Moreover, local variability could partially explain why the relationship between SST and adult length is different in other regions of the CCE (Robertson and Bjorkstedt, 2020).

Regional differences in krill length response to environmental variability may be key to understanding how ocean warming will impact this numerically and trophically important taxon. Spatial and temporal fluctuations in krill biomass during the 2014–2016 MHW have been linked to seabird reproductive failures (Jones et al., 2018), reduced fishery recruitment (McClatchie et al., 2016) and increased whale mortality (Santora et al., 2020). In turn, indirect effects of the MHW on krill predators have had system-wide ecological and socioeconomic consequences. Future studies could expand on our work by investigating regional variation in the

response of krill biomass response to environmental change, perhaps identifying high-risk locations where krill are particularly sensitive to warming or refugia that help to mitigate the effects of extreme climate events for both krill and their predators. These insights may prove invaluable for managers seeking to enact ecosystem-based fishery management in the region (Harvey et al., 2019).

CONCLUSION

We demonstrated that the observed 2014–2016 Northeast Pacific MHW/El Niño had a strong impact on the adult body size of three common krill species in the CCE, particularly in 2015 (no length data available for 2014). Adult krill length declined for two temperate species (*E. pacifica* and *T. spinifera*) adapted to cool, highly productive waters, but increased for one temperate–subtropical species (*N. difficilis*) adapted to warmer conditions. We also show evidence that female size declined relative to male size for all three species, indicating that heatwave conditions made reproductive energy allocation more costly to females in terms of somatic growth. Finally, we found that high SST and low upwelling and primary productivity were not strong predictors of reduced krill size during 2014–2016, but drivers of krill size appear to vary by location providing early evidence that some locations may serve as refugia for krill from the worst effects of extreme climate events. Making multispecific comparisons across large spatial and long temporal scales is a powerful approach that provided new insights into the effect of extreme climate events and environmental drivers on krill populations with cascading consequences for key predators in pelagic ecosystems. Our observations offer a guide to how we may expect krill biomass to be impacted by future climate change, including the increasing frequency of MHWs (Frölicher et al., 2018).

Funding

This project was supported by funding from California Sea Grant (project number R/SFA-03).

Data availability statement

The data underlying this article are available in a GitHub repository available at <https://doi.org/10.17605/osf.io/c8hr3>.

Supplementary data

Supplementary materials including metadata, supporting figures, and additional statistical analysis are available at the ICESJMS online version of the manuscript.

Author contributions

Study conception and design: H. Killeen, J. Dorman, W. Sydeman, C. Dibble, and S. Morgan.

Acquisition of data: H. Killeen, C. Dibble, and S. Morgan.

Analysis and interpretation of data: H. Killeen, C. Dibble, J. Dorman, and W. Sydeman.

Drafting of manuscript: H. Killeen.

Critical revision: H. Killeen, J. Dorman, S. Morgan, C. Dibble, and W. Sydeman.

Acknowledgements

We thank Baldo Marinovic and the members of the NOAA-NMFS RREAS team for collection of and access to krill samples and meta-data. We also thank Sadie Small and the many students and researchers who assisted in identifying and measuring krill at Bodega Marine Laboratory including Ian Brown, Mrudula Chodavarapu, Hailey Gleason, Anna Groehnert, Eduardo Hernandez, Haley Hudson, Andy Lee, Joe Lozano, Armand McFarland, Alma Meckler, Gynelle Mendoca, Roshni Mangar, Chloe Parish, Giovanna Poulos, Niko Schoffer, Ava Smith, Eda Spaletta, Anya Stajner, Rafael Stankiewicz, Claire Sydeman, Laura Vary, and Jeffrey You. Finally, we thank Kate Hewett, Marisol García-Reyes, and Chelle Gentemann for assistance with environmental datasets; Andrew Latimer and UC Davis Statistical Consulting for statistical advice; and Ellie Bolas, John Field, and five anonymous reviewers for helpful editing.

References

- Alonzo, S., and Mangel, M. 2001. Survival strategies and growth of krill: avoiding predators in space and time. *Marine Ecology Progress Series*, 209: 203–217.
- Baker, A. d. C., Boden, B., and Brinton, E. 1990. *A Practical Guide to the Euphausiids of the World*, Natural History Museum Publications, London.
- Barlow, D. R., Bernard, K. S., Escobar-Flores, P., Palacios, D. M., and Torres, L. G. 2020. Links in the trophic chain: modeling functional relationships between in situ oceanography, krill, and blue whale distribution under different oceanographic regimes. *Marine Ecology Progress Series*, 642: 207–225.
- Barter, R., and Yu, B. 2017. superheat: a graphical tool for exploring complex datasets using heatmaps. <https://cran.r-project.org/web/packages/superheat/index.html>. Accessed 15 Oct 2021.
- Bartón, K. 2020. MuMIn: multi-model inference. <https://cran.r-project.org/web/packages/MuMIn/index.html>. Accessed 15 Oct 2021.
- Bates, D., Mächler, M., Bolker, B., and Walker, S. 2015. Fitting linear mixed-effects models using lme4. *Journal of Statistical Software*, 1: 51.
- Bond, N. A., Cronin, M. F., Freeland, H., and Mantua, N. 2015. Causes and impacts of the 2014 warm anomaly in the NE Pacific. *Geophysical Research Letters*, 42: 3414–3420.
- Brinton, E. 1960. Changes in the distribution of euphausiid crustaceans in the region of the California Current. *California Cooperative Oceanic Fisheries Investigations Reports*, 7: 137–146.
- Brinton, E. 1962. The distribution of Pacific euphausiids. *Bulletin of the Scripps Institution of Oceanography*, 8: 21–270.
- Brinton, E., Ohman, M. D., Townsend, A., Knight, M. D., and Bridgeman, A. L. 2000. *Euphausiids of the World Oceans, Series: World Biodiversity Database CD-ROM Series*, Expert Center for Taxonomic Identification. Springer, Amsterdam, Netherlands.
- Brinton, E., and Townsend, A. 2003. Decadal variability in abundances of the dominant euphausiid species in southern sectors of the California Current. *Deep Sea Research Part II Topical Studies in Oceanography*, 50: 2449–2472.
- Brinton, E., and Wyllie, J. G. 1976. *Distributional Atlas of Euphausiid Growth Stages off Southern California, 1953–1956*. Marine Life Research Program, Scripps Institution of Oceanography. 24.
- Brodeur, R. D., Auth, T. D., and Phillips, A. J. 2019. Major shifts in pelagic micronekton and macrozooplankton community structure in an upwelling ecosystem related to an unprecedented marine heatwave. *Frontiers in Marine Science*, 6: 212.
- Checkley, D. M., and Barth, J. A. 2009. Patterns and processes in the California Current System. *Progress in Oceanography*, 83: 49–64.
- Cimino, M. A., Santora, J. A., Schroeder, I., Sydeman, W., Jacox, M. G., Hazen, E. L., and Bograd, S. J. 2020. Essential krill species habitat resolved by seasonal upwelling and ocean circulation models within the large marine ecosystem of the California Current System. *Ecography*, 43: 1536–1549.
- Di Lorenzo, E., and Mantua, N. 2016. Multi-year persistence of the 2014/15 North Pacific marine heatwave. *Nature Climate Change*, 6: 1042–1047.
- Dilling, L., Wilson, J., Steinberg, D., and Alldredge, A. 1998. Feeding by the euphausiid *Euphausia pacifica* and the copepod *Calanus pacificus* on marine snow. *Marine Ecology Progress Series*, 170: 189–201.
- Feinberg, L. R., and Peterson, W. T. 2003. Variability in duration and intensity of euphausiid spawning off central Oregon, 1996–2001. *Progress in Oceanography*, 57: 363–379.
- Feinberg, L. R., Peterson, W. T., and Tracy Shaw, C. 2010. The timing and location of spawning for the Euphausiid *Thysanoessa spinifera* off the Oregon coast, USA. *Deep Sea Research Part II Topical Studies in Oceanography*, 57: 572–583.
- Feinberg, L. R., Shaw, C. T., and Peterson, W. T. 2007. Long-term laboratory observations of *Euphausia pacifica* fecundity: comparison of two geographic regions. *Marine Ecology Progress Series*, 341: 141–152.
- Field, J. C., and Francis, R. C. 2006. Considering ecosystem-based fisheries management in the California Current. *Marine Policy*, 30: 552–569.
- Field, J. C., Francis, R. C., and Aydin, K. 2006. Top-down modeling and bottom-up dynamics: linking a fisheries-based ecosystem model with climate hypotheses in the Northern California Current. *Progress in Oceanography*, 68: 238–270.
- Fleming, A. H., Clark, C. T., Calambokidis, J., and Barlow, J. 2016. Humpback whale diets respond to variance in ocean climate and ecosystem conditions in the California Current. *Global Change Biology*, 22: 1214–1224.
- Frölicher, T. L., Fischer, E. M., and Gruber, N. 2018. Marine heatwaves under global warming. *Nature*, 560: 360–364.
- García-Reyes, M., Largier, J. L., and Sydeman, W. J. 2014. Synoptic-scale upwelling indices and predictions of phyto- and zoo-plankton populations. *Progress in Oceanography*, 120: 177–188.
- García-Reyes, M., and Sydeman, W. J. 2017. California Multivariate Ocean Climate Indicator (MOCI) and marine ecosystem dynamics. *Ecological Indicators*, 72: 521–529.
- Gelman, A., and Hill, J. 2007. *Data Analysis Using Regression and Multilevel/hierarchical Models*, Cambridge University Press, Cambridge, UK.
- Gentemann, C. L., Fewings, M. R., and García-Reyes, M. 2017. Satellite sea surface temperatures along the West Coast of the United States during the 2014–2016 northeast Pacific marine heat wave. *Geophysical Research Letters*, 44: 312–319.
- Gómez-Gutiérrez, J., Feinberg, L. R., Shaw, C., and Peterson, W. 2006. Variability in brood size and female length of *Euphausia pacifica* among three populations in the North Pacific. *Marine Ecology Progress Series*, 323: 185–194.
- Grueber, C. E., Nakagawa, S., Laws, R. J., and Jamieson, I. G. 2011. Multimodel inference in ecology and evolution: challenges and solutions. *Journal of Evolutionary Biology*, 24: 699–711.
- Harvey, C., Garfield, N., Williams, G., Tolimieri, N., Schroeder, I., Andrews, K., Barnas, K. *et al.* 2019. Ecosystem status report of the California Current for 2019: a summary of ecosystem indicators compiled by the California Current Integrated Ecosystem Assessment team (CCIEA). NOAA Technical Memorandum NMFS-NWFSC-149. National Marine Fisheries Service. Northwest Region.
- Hipfner, J. M. 2009. Euphausiids in the diet of a North Pacific seabird: annual and seasonal variation and the role of ocean climate. *Marine Ecology Progress Series*, 390: 277–289.
- Hobday, A. J., Alexander, L. V., Perkins, S. E., Smale, D. A., Straub, S. C., Oliver, E. C. J., Benthuisen, J. A. *et al.* 2016. A hierarchical approach to defining marine heatwaves. *Progress in Oceanography*, 141: 227–238.
- Iguchi, N., and Ikeda, T. 1995. Growth, metabolism and growth efficiency of a euphausiid crustacean *Euphausia pacifica* in the southern Japan Sea, as influenced by temperature. *Journal of Plankton Research*, 17: 1757–1769.
- Jacox, M. G., Edwards, C. A., Hazen, E. L., and Bograd, S. J. 2018. Coastal upwelling revisited: ekman, Bakun, and improved upwelling

- indices for the U.S. West Coast. *Journal of Geophysical Research: Oceans*, 123: 7332–7350.
- Jones, T., Parrish, J. K., Peterson, W. T., Bjorkstedt, E. P., Bond, N. A., Ballance, L. T., Bowes, V. *et al.* 2018. Massive mortality of a planktivorous seabird in response to a marine heatwave. *Geophysical Research Letters*, 45: 3193–3202.
- Koehn, L. E., Essington, T. E., Marshall, K. N., Kaplan, I. C., Sydeman, W. J., Szoboszlai, A. I., and Thayer, J. A. 2016. Developing a high taxonomic resolution food web model to assess the functional role of forage fish in the California Current ecosystem. *Ecological Modelling*, 335: 87–100.
- Krag, L. A., Herrmann, B., Iversen, S. A., Engås, A., Nordrum, S., and Krafft, B. A. 2014. Size selection of Antarctic krill (*Euphausia superba*) in trawls. *Plos ONE*, 9: e102168.
- Lavaniegos, B. E., Jiménez-Herrera, M., and Ambriz-Arreola, I. 2019. Unusually low euphausiid biomass during the warm years of 2014–2016 in the transition zone of the California Current. *Deep Sea Research Part II Topical Studies in Oceanography*, 169–170: 104638.
- Lilly, L. E., and Ohman, M. D. 2021. Euphausiid spatial displacements and habitat shifts in the southern California Current System in response to El Niño variability. *Progress in Oceanography*, 193: 102544.
- Marinovic, B., and Mangel, M. 1999. Krill can shrink as an ecological adaptation to temporarily unfavourable environments. *Ecology Letters*, 2: 338–343.
- Marinovic, B. B., Croll, D. A., Gong, N., Benson, S. R., and Chavez, F. P. 2002. Effects of the 1997–1999 El Niño and La Niña events on zooplankton abundance and euphausiid community composition within the Monterey Bay coastal upwelling system. *Progress in Oceanography*, 54: 265–277.
- McClatchie, S., Goericke, R., Leising, A., Auth, T. D., Bjorkstedt, E., Robertson, R., Brodeur, R. *et al.* 2016. State of the California Current 2015–16: comparisons with the 1997–98 El Niño. *California Cooperative Oceanic Fisheries Investigations Reports*, 57: 5–61.
- Nakagawa, Y., Ota, T., Endo, Y., Taki, K., and Sugisaki, H. 2004. Importance of ciliates as prey of the euphausiid *Euphausia pacifica* in the NW North Pacific. *Marine Ecology Progress Series*, 271: 261–266.
- Nemoto, T. 1966. *Thysanoessa* euphausiids, comparative morphology, allomorphy and ecology. *Scientific Reports of the Whales Research Institute*, 20: 109–155.
- Nickels, C. F., Sala, L. M., and Ohman, M. D. 2018. The morphology of euphausiid mandibles used to assess selective predation by blue whales in the southern sector of the California Current System. *Journal of Crustacean Biology*, 38: 563–573.
- Ohman, M. D. 1984. Omnivory by *Euphausia pacifica*: the role of copepod prey. *Marine Ecology Progress Series*, 19: 125–131.
- Piatt, J. F., Parrish, J. K., Renner, H. M., Schoen, S. K., Jones, T. T., Arimitsu, M. L., Kuletz, K. J. *et al.* 2020. Extreme mortality and reproductive failure of common murrelets resulting from the northeast Pacific marine heatwave of 2014–2016. *Plos ONE*, 15: e0226087.
- Pinchuk, A. I., and Hopcroft, R. R. 2007. Seasonal variations in the growth rates of euphausiids (*Thysanoessa inermis*, *T. spinifera*, and *Euphausia pacifica*) from the northern Gulf of Alaska. *Marine Biology*, 151: 257–269.
- Pond, D., Watkins, J., Priddle, J., and Sargent, J. 1995. Variation in the lipid content and composition of Antarctic krill *Euphausia superba* at South Georgia. *Marine Ecology Progress Series*, 117: 49–57.
- R Core Team 2019. R: a language and environment for statistical computing. Vienna, Austria.
- Robertson, R. R., and Bjorkstedt, E. P. 2020. Climate-driven variability in *Euphausia pacifica* size distributions off northern California. *Progress in Oceanography*, 188: 102412.
- Ross, R., and Quetin, L. 2000. Reproduction in Euphausiacea. *In* *Krill: Biology, Ecology and Fisheries*. Ed. by Everson, I., Blackwell Science, Cambridge, UK.
- Rueden, C., Schindelin, J., Hiner, M., DeZonia, B., Walter, A., and Elieceiri, K. 2017. ImageJ2: imageJ for the next generation of scientific image data. *BMC Bioinformatics*, 18: 529.
- Sakuma, K. M., Field, J. C., Mantua, N. J., Ralston, S., Marinovic, B. B., and Carrion, C. N. 2016. Anomalous epipelagic micronekton assemblage patterns in the neritic waters of the California Current in spring 2015 during a period of extreme ocean conditions. *California Cooperative Oceanic Fisheries Investigations Reports*, 57: 163–183.
- Sakuma, K. M., Ralston, S., and Weststad, V. G. 2006. Interannual and spatial variation in the distribution of young-of-the-year rockfish (*Sebastes spp.*): expanding and coordinating a survey sampling frame. *California Cooperative Oceanic Fisheries Investigations Reports*, 47: 127–139.
- Santora, J. A., Mantua, N. J., Schroeder, I. D., Field, J. C., Hazen, E. L., Bograd, S. J., Sydeman, W. J. *et al.* 2020. Habitat compression and ecosystem shifts as potential links between marine heatwave and record whale entanglements. *Nature Communications*, 11: 536.
- Sathyendranath, S., Jackson, T., Brockmann, C., Brotas, V. C., Chuprin, A. B., Clements, O., Cipollini, P. *et al.* 2020. ESA Ocean Colour Climate Change Initiative (Ocean_Colour_cci): Global chlorophyll-a data products gridded on a sinusoidal projection, version 4.2. Centre for Environmental Data Analysis.
- Shaw, C., Peterson, W., and Feinberg, L. 2010. Growth of *Euphausia pacifica* in the upwelling zone off the Oregon coast. *Deep Sea Research Part II Topical Studies in Oceanography*, 57: 584–593.
- Shaw, C. T., Bi, H., Feinberg, L. R., and Peterson, W. T. 2021. Cohort analysis of *Euphausia pacifica* from the Northeast Pacific population using a Gaussian mixture model. *Progress in Oceanography*, 191: 102495.
- Smiles, M. C., and Percy, W. G. 1971. *Fisheries Bulletin*, 69: 79–86.
- Sydeman, W. J., Thompson, S. A., Santora, J. A., Koslow, J. A., Goericke, R., and Ohman, M. D. 2015. Climate–ecosystem change off southern California: time-dependent seabird predator–prey numerical responses. *Deep Sea Research Part II Topical Studies in Oceanography*, 112: 158–170.
- Tanasichuk, R. W. 1998a. Interannual variations in the population biology and productivity of *Euphausia pacifica* in Barkley Sound, Canada, with special reference to the 1992 and 1993 warm ocean years. *Marine Ecology Progress Series*, 173: 163–180.
- Tanasichuk, R. W. 1998b. Interannual variations in the population biology and productivity of *Thysanoessa spinifera* in Barkley Sound, Canada, with special reference to the 1992 and 1993 warm ocean years. *Marine Ecology Progress Series*, 173: 181–195.
- Thayer, J. A., Field, J. C., and Sydeman, W. J. 2014. Changes in California Chinook salmon diet over the past 50 years: relevance to the recent population crash. *Marine Ecology Progress Series*, 498: 249–261.
- Trathan, P. N., and Hill, S. L. 2016. The importance of krill predation in the Southern Ocean. *In* *Biology and ecology of Antarctic krill*, 1st edn. Ed. by Seigel, V., Springer International, Switzerland.
- Wells, B. K., Santora, J. A., Schroeder, I. D., Mantua, N., Sydeman, W. J., Huff, D. D., and Field, J. C. 2016. Marine ecosystem perspectives on Chinook salmon recruitment: a synthesis of empirical and modeling studies from a California upwelling system. *Marine Ecology Progress Series*, 552: 271–284.
- Wickham, H. 2016. ggplot2: elegant graphics for data analysis: <https://cran.r-project.org/package=ggplot2>. Accessed 15 Oct 2021.
- Zhu, H. 2020. kableExtra: construct complex table with 'kable' and pipe syntax: <https://cran.r-project.org/package=kableExtra>. Accessed 15 Oct 2021.